SSC18-PII-26

Control of Long-Term Low-Thrust Small Satellites Orbiting Mars

Christopher Swanson
University of Florida
3131 NW 58th Blvd. Gainesville FL
ccswanson@ufl.edu

Faculty Advisor: Riccardo Bevilacqua **Graduate Advisor:** Patrick Kelly
University of Florida

ABSTRACT

As expansion of deep space missions continue, Mars is quickly becoming the planet of primary focus for science and exploratory satellite systems. Due to the cost of sending large satellites equipped with enough fuel to last the entire lifespan of a mission, inexpensive small satellites equipped with low thrust propulsion are of continuing interest. In this paper, a model is constructed for use in simulating the control of a small satellite system, equipped with low-thrust propulsion in orbit around Mars. The model takes into consideration the fuel consumption and can be used to predict the lifespan of the satellite based on fuel usage due to the natural perturbation of the orbit. This model of the natural perturbations around Mars implements a Lyapunov Based control law using a set of gains for the orbital elements calculated by obtaining the ratio of the instantaneous rate of change of the element over the maximum rate of change over the current orbit. The thrust model simulates the control of the semi-major axis, eccentricity, and inclination based upon a thrust vector fixed to a local vertical local horizontal reference frame of the satellite. This allows for a more efficient fuel usage over the long continuous thrust burns by prioritizing orbital elements in the control when they have a higher relative rate of change rather than the Lyapunov control prioritizing the element with the greatest magnitude rate of change.

INTRODUCTION

The increased commercial interest in space exploration has driven a highly cost focused approach to satellite development. Small satellites, such as Cube-Satellites, offer a solution in the form of a focused compact design. These systems require smaller and simpler propulsion systems to enter and maintain a mission orbit. Due to the weight and size concerns of carrying large amounts of fuel, low-thrust high specific impulse systems, such as electric gridded ion or hall-effect thrusters, are commonly chosen for these missions.[5]

Short term deep space test satellites such as Mars Cube One[5] in addition to cube-sat verification missions RAX-1 and RAX-2[6] are being launched, coupled with larger missions, to test the electronic systems on these satellites in the environment of deep space. As these experiments conclude, the next step will be to construct longer life-span missions to utilize the unique cost and size considerations of small satellites.

Satellites requiring orbital control typically use a linearized system, such as LQR, to ensure stability and controllability of the system.[7] These control systems are simpler to implement and analyze compared to non-linear controllers, while also serving as robust approximations for most dynamic systems. Due to inclusions of natural spherical harmonics perturbations over large time spans in this paper's Mars model, a non-linear Lyapunov controller is implemented to preserve these non-linear dynamics.

The control of electric propulsion systems on a small-satellite frame such as a Cube-Sat can be challenging due to the large time spans of the continuous burns required to achieve final orbits, while maintaining the cost and fuel goals due to the limited resources available on a small satellite. The Lyapunov control method can be used a set gain, either static or variable, for each of the elements being controlled, which can be determined in several different ways analytically or experimentally.[3] These gains must be used carefully as they can make a stable Lyapunov function become unstable.

In this document, a verification of a Lyapunov thrust control is outlined and simulated to investigate if a theoretical small-satellite can utilize a low-thrust propulsion system for a long-term Mars based mission. A MATLAB based simulation was constructed to analyze different orbit maneuvers, with different low-thrust spacecraft, to verify if a certain engine and satellite mass configuration achieves fuel efficiency and time-

based objectives. This also allows the measurement of the fuel usage of different maneuvers in a Mars centered system.

Sec. II demonstrates the effect the separate components of the natural perturbation model have on the orbital element drift and therefore the maintenance of the targeted orbital elements of a small satellite around Mars. Sec. III provides a method of verification of a Lyapunov based control with gains based on the efficiency of a control perturbation on the rate of change of an orbit parameter.

ORBIT SIMULATION DYNAMICS MODEL

Reference Frames and Coordinate Systems

For the purposes of a Mars focused orbit simulation three reference frames are chosen and four coordinate systems are constructed to define and measure the motion and relative position of the satellite around Mars. In addition, the satellite can also be described in terms of classical orbital element around Mars.

The Inertial frame used is the Mars Centered Inertial (MCI) frame which is based around Mars but does not rotate with Mars. It is fixed instead to the ICRF frame's rotation much as the J2000 frame is for an Earth Centered Inertial frame. This allows us to treat it as an inertial reference frame for measurements in Mars' orbit. A coordinate system is constructed in this frame with the origin at the center of mars and the primary axis in the direction of the vector formed by the intersection of the Mars mean equator with the Earth mean equator[4] with the normal axis being in the direction of the vector normal to the Mars mean equatorial plane and the third axis **{j}** is the normal axis direction **{k}** crossed with the primary axis direction **{i}**.

The planet fixed reference frame is the Mars Centered Mars Fixed (MCMF) frame, which rotates with the same rotational velocity of mars as to remain fixed to its surface. The Coordinate system fixed in the MCMF frame is centered with an origin at the center of the planet and the primary axis **{x}** is in the direction of the point on the surface of the planet the Mars Centered Inertial coordinate system's primary axis passes through at the J2000 epoch. The normal axis **{z}** is the vector normal to the mean equatorial plane of Mars and the third axis **{y}** is the normal vector crossed with the primary vector.

Two useful satellite centered coordinate systems are constructed named RSW and VNC that are fixed in the satellite body reference frame. RSW has primary axis **{R}** which is the direction of the position of the satellite relative to the center of the planet with W being the direction of the vector normal to the plane of the orbit and the third direction **{S} = W×R**. The VNC frame has primary axis V in the direction of the velocity relative to the center of Mars with the direction N is the direction of the vector normal to the orbit plane and the third direction **{C}=V×N**.

The description of the state of the satellite with respect to Mars are initialized in classical orbital element notation and are converted to a MCI coordinate system cartesian position and velocity **{i, j, k}** to enable a numerical ordinary differential equation solver to solve for the states given equations of motion and perturbations for those states in the MCI frame.

Mars Two Body Spherical Harmonic Effect

When considering the orbit of any object around a planet the largest and first effect to include is the effect of the standard two body Keplerian acceleration due to the point mass approximation of the larger body (1), with μ being the gravitational parameter and **r** being the position of the orbiting body relative to the center of the planet.

$$\ddot{\boldsymbol{r}} = -\frac{\mu}{r^3}\boldsymbol{r} \tag{1}$$

Where r = the magnitude of position of the orbiting satellite; μ = gravitational parameter; and **r** = the vector position of the orbiting satellite. This equation uses two major assumptions to simplify the result:

1) The mass of the orbiting body is many orders of magnitude smaller than the planet.

2) The planet is a perfectly spherical body with constant gravity across its surface.

This model is for a satellite whose mass is many orders of magnitude smaller than the mass of Mars, therefore the first assumption is still necessary and valid. The simplification of Mars to a perfect spheroid could cause problems over the time spans being modeled, so a model of the effect of these oblateness deviations from the assumption of a perfect sphere needs to be constructed.

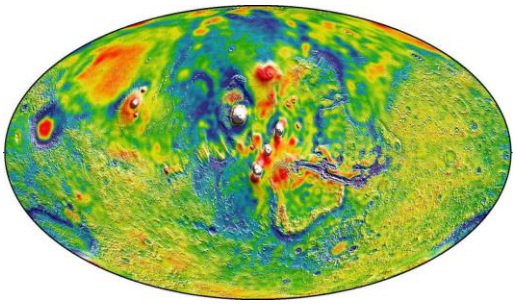

Figure 1. GMM-3 Map of gravity gradients

The Goddard Space Flight Center has constructed such a model from the data of Mars Global Surveyor (MGS), Mars Odyssey (ODY), and the Mars Reconnaissance Orbiter (MRO) called the Goddard Mars Model 3 (GMM3).[1] The variation seen in the map of gravity gradients shows large localized effects from mountain ranges and crustal variations. These effects can be modeled using a series of coefficients in a geopotential model called zonal and tesseral spherical harmonic coefficients using an altered form of the equation for the two body Keplerian acceleration in the MCMF coordinate system **{a_x, a_y, a_z}** after converting the position of the satellite back from the a spherical coordinate system **{r, λ, ϕ}** to a cartesian MCMF coordinate system **{x, y, z}** to simplify the expression for the potential of the satellite around Mars.[2]

$$a_{x,y,z} = \frac{\partial}{\partial r_{x,y,z}}\left\{-\frac{\mu}{r}\left[1+\sum_{l=2}^{\infty}\sum_{m=0}^{l}\left(\frac{R}{r}\right)^{l} P_{l,m}\sin(\varphi)\{C_{l.m}\cos(m\lambda) + S_{l,m}\sin(m\lambda)\}\right]\right\} \quad (2)$$

Where R = radius of mars; $P_{l,m}$ = the associated Legendre function; $S_{l,m}$ and $C_{l,m}$ = coefficients based upon experimental measurements; l and m = order of the harmonics modeled. This equation obtains the acceleration perturbations, or the Geopotential acceleration, due to the planet including the effects of the aspherical properties of the planet up to an order n = l = m using the coefficients obtained from the GMM3 model. For the purposes of numerical solution Geopotential effects up to order 5 were used, as any effects from higher orders were found to be obscured by native machine error.

Third Body Effects

The major third body perturbation effects on a satellite orbiting Mars come from the gravity of Mar's two moons, Phobos and Deimos, and the Sun. The effects from other objects in the solar system were found to have negligible influence on the position and motion of the satellite. We can use the expression for a three-body system isolating the effect from just the third body.

$$\ddot{\boldsymbol{r}}_{sat} + \frac{\mu}{r_{sat}^3}\boldsymbol{r}_{sat} = \mu_3\left[\boldsymbol{r}_{sat} - 3r_3\frac{\boldsymbol{r}_{sat}\cdot\boldsymbol{r}_3}{r_3^2} - \frac{15}{2}\left(\frac{\boldsymbol{r}_{sat}\cdot\boldsymbol{r}_3}{r_3^2}\right)^2\boldsymbol{r}_3\right] \quad (3)$$

This allows the third body gravity effects from the moons and Sun to be numerically calculated in the inertial MCI frame using a single expression and added to the final expression for the Geopotential acceleration due to Mars.[2]

Numerical Solution for the uncontrolled system

The constructed model of the gravity effects perturbing the satellite are the equations of motion for the satellite. These equations can be solved over time using MATLAB or a similar numerical integrator. This will result in an array of states describing the position and velocity of the satellite in the inertial frame. For analysis of the gravity effects, the results of the uncontrolled systems will be converted to orbital elements over the span of one Martian year (~687 Earth days). The example coasting simulation starts at an arbitrary Areosynchronus orbit (20427 kilometers semi-major axis) with 45 degrees inclination. The uncontrolled system simulation can be analyzed to provide a clear picture of how the different natural perturbations of the satellite's orbit affect the systems controllability and orbital elements over time.

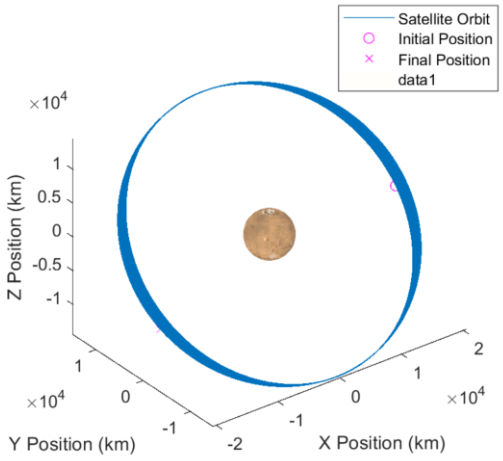

Figure 2. Coasting Orbit around Mars.

As can be seen in the Fig. 3 for this example, the semi-major axis experiences an oscillation of constant magnitude of 30km with a period of approximately 180 days which is mostly due to the Geopotential variations from Mars, as when the third body gravity effects are remove the system's semi-major axis oscillates nearly identically.

The inclination oscillates with what looks like a relatively large then relatively small magnitude, which then repeats once over the year long time scale, while the eccentricity has a high frequency noisy oscillation that tends to increase over time. Each of these oscillations or trends in the orbital elements can be isolated by selectively removing parts of the gravity model (e.g. remove the third body effect from the Sun to see that the eccentricity increasing trend nearly disappears) to determine how each natural perturbation tends to affect

the system. This method is also useful for determining the order at which the Geopotential model should be set at by selecting the order for which any higher order would not noticeably change the system.

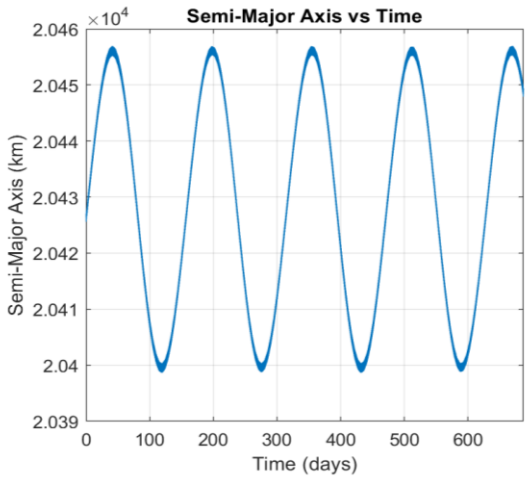

Figure 3. Semi-Major Axis oscillating over a one year time span due to the Spherical Harmonics of Mars caused by mountainous regions and crustal variations.

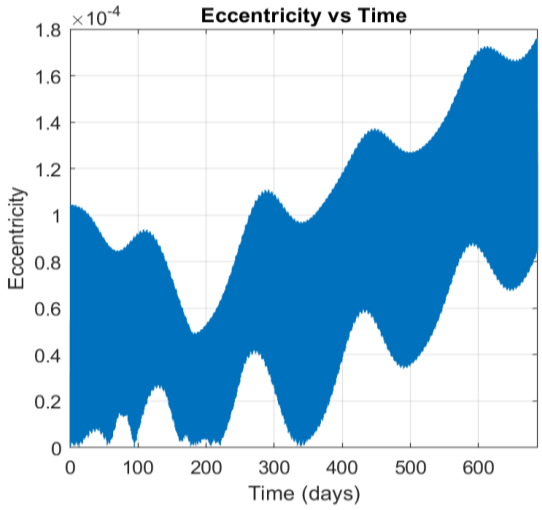

Figure 3. Small eccentricity variations increasing slowly over time mostly due to Solar gravity acting on the satellite.

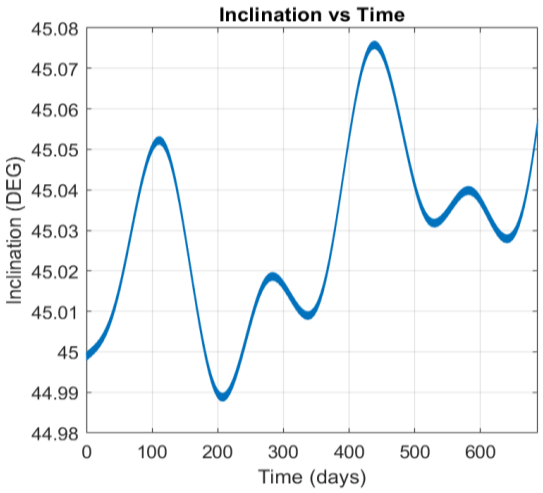

Figure 3. Inclination changes over a one year time span caused by a number of factors including the moons, Phobos and Deimos, and the sun.

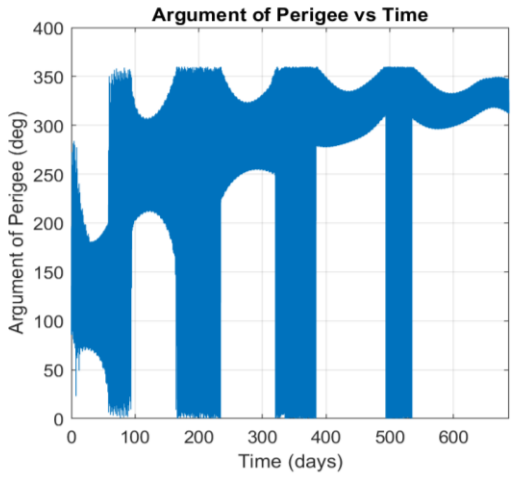

Figure 3. Argument of perigee variations caused by all natural perturbations.

CONTROLLED SYSTEM

Equations and State

The state of the satellite is stored as a position and velocity with respect to the mars inertial frame (MCI) and can be converted from position and velocity (RV) parameters to classical Keplerian elements and vice versa. This allows the use of the Gauss variation equations[2] to find the rate of change in these parameters due to perturbations in the satellites orbit.

$$\frac{da}{dt} = \frac{2}{n\sqrt{1-e^2}}\left\{\text{esin}(\nu)\, F_R + \frac{p}{r} F_S\right\} \tag{4}$$

$$\frac{de}{dt} = \frac{\sqrt{1-e^2}}{na}\left\{\sin(\nu)\, F_R + \left(\cos(\nu) + \frac{e+\cos(\nu)}{1+e\cos(\nu)}\right) F_S\right\} \tag{5}$$

$$\frac{di}{dt} = \frac{\text{rcos}(u)}{na^2\sqrt{1-e^2}} F_w \tag{6}$$

$$\frac{d\Omega}{dt} = \frac{\text{rsin}(u)}{na^2\sqrt{1-e^2}\sin(i)} F_w \tag{7}$$

$$\frac{d\omega}{dt} = \frac{\sqrt{1-e^2}}{nae}\left\{-\cos(\nu) F_R + \sin(\upsilon)\left(1+\frac{r}{p}\right) F_S\right\} - \frac{r\cot(i)\sin(u)}{h} F_w \tag{8}$$

$$\frac{d\nu}{dt} = \frac{\sqrt{1-e^2}}{nae}\cos(\upsilon)\, F_R - \frac{\sqrt{1-e^2}}{nae}\frac{2+\text{ecos}(\nu)}{1+\text{ecos}(\nu)} F_S \tag{9}$$

Where a = semi-major axis; e = eccentricity; i = inclination; Ω = right ascension of the ascending node; ω = argument of periapsis; ν = true anomaly; h = magnitude of the angular acceleration; n = mean motion; u = argument of latitude; and F_R, F_S, and F_W are the perturbing forces in the {R,S,W} directions respectively.[2]

Control Via Lyapunov Function

The system for the time rate of change of the orbital elements can be modeled as solely dependent on ta function of the current values of the orbital elements and time summed with the RSW reference frame control accelerations **u (u_R, u_S, u_W)** multiplied by some input matrix **A**.

The change in the orbital elements $\boldsymbol{O}$ over time can be modeled in equation 10 as a function of time and a control perturbation to the system $\boldsymbol{u}$.

$$\dot{\boldsymbol{O}} = \boldsymbol{f}(\boldsymbol{O}, \boldsymbol{t}) + \boldsymbol{A}\boldsymbol{u} \tag{10}$$

In equation 11, the Gauss Variational equations can be constructed as an input matrix $\boldsymbol{A}$ for semi-major axis, inclination, and eccentricity.

$$\boldsymbol{A} = \begin{bmatrix} \frac{2\,\text{esin}(\nu)}{n\sqrt{1-e^2}} & \frac{2p}{rn\sqrt{1-e^2}} & 0 \\ \frac{\sin(\nu)\sqrt{1-e^2}}{na} & \frac{\sqrt{1-e^2}}{na}\left(\cos(\nu) + \frac{e+\cos(\nu)}{1+e\cos(\nu)}\right) & 0 \\ 0 & 0 & \frac{\text{rcos}(u)}{na^2\sqrt{1-e^2}} \end{bmatrix} \tag{11}$$

As derived by Naasz [3], a candidate Lyapunov function $V(\boldsymbol{Au}) = \frac{1}{2}(\boldsymbol{Au})^T(\boldsymbol{Au})$ yields a control law $\boldsymbol{u}$

$$\boldsymbol{u} = -\boldsymbol{A}^T\boldsymbol{K}\boldsymbol{e} \tag{10}$$

with the set of gains $\boldsymbol{K}$

$$\boldsymbol{K}\boldsymbol{e} = \begin{bmatrix} K_a \\ K_e \\ K_i \end{bmatrix}\begin{bmatrix} (a - a_{desired}) \\ (e - e_{desired}) \\ (i - i_{desired}) \end{bmatrix}^T \tag{11}$$

for the required control thruster accelerations to minimize the error matrix $\boldsymbol{e}$.

Efficiency Gains

The gain matrix K allows the user control over the system to obtain results that cater to the needs of an orbit transfer or maintenance of the targeted orbit, such as fuel efficiency or maintaining one of the orbital elements at the expense of the others. The gains chosen for the general case are based on the efficiency of the rate of change of the associated element for the current true anomaly of the current orbit. This is done by obtaining the ratio of the current rate of change of the controlled orbital elements **($\delta a/\delta t$)** to the maximum rate of change **$(\delta a/\delta t)_{max}$** for the current orbit across all true anomaly values.

$$\begin{bmatrix} \frac{\partial a}{\partial t}\left(\frac{\partial a}{\partial t}\right)^{-1}_{max} \\ \frac{\partial e}{\partial t}\left(\frac{\partial e}{\partial t}\right)^{-1}_{max} \\ \frac{\partial i}{\partial t}\left(\frac{\partial i}{\partial t}\right)^{-1}_{max} \end{bmatrix} = \begin{bmatrix} \frac{\left\{\text{esin}(\nu) + \frac{p}{r}\right\}}{\left\{\text{esin}(\nu_{max}) + \frac{p}{r_{max}}\right\}} \\ \frac{\left\{\sin(\nu) + \left(\cos(\nu) + \frac{e+\cos(\nu)}{1+\text{ecos}(\nu)}\right)\right\}}{\left\{\sin(\nu_{max}) + \left(\cos(\nu_{max}) + \frac{e+\cos(\nu_{max})}{1+e\cos(\nu_{max})}\right)\right\}} \\ \frac{\text{rcos}(u)}{\text{r}_{\max}\cos(u_{max})} \end{bmatrix} \tag{12}$$

This results in a gain matrix $\boldsymbol{K}$, where S is a scale factor to normalize the elements for the control and K_a, K_e, and K_i are the gains of the semi-major axis, eccentricity, and inclination respectively.

$$\boldsymbol{K} = \begin{bmatrix} K_a \\ K_e \\ K_i \end{bmatrix} = \begin{bmatrix} S_a \frac{\partial a}{\partial t}\left(\frac{\partial a}{\partial t}\right)^{-1}_{max} \\ S_a \frac{\partial e}{\partial t}\left(\frac{\partial e}{\partial t}\right)^{-1}_{max} \\ S_a \frac{\partial i}{\partial t}\left(\frac{\partial i}{\partial t}\right)^{-1}_{max} \end{bmatrix} \tag{13}$$

The simplifying assumption of the thrust force components being the same magnitude in the ratio allows for a numerically determine gain to be calculated for every state in the system. The maximum terms are found by solving the system bound by [0,2π] for the values $\nu_{max}, \text{r}_{\max}, u_{max}$ which result in the largest rate of change of the elements. This gain matrix allows for the

conservation of fuel during periods of the orbit that are relatively inefficient true anomalies for thruster burns to reduce the current error in the system.

Example of a Controlled Transfer with the Constructed Efficiency Gains

The following test maneuver chosen is a transfer from an injection orbit to a circular AEO (Areosynchronus Orbit) orbit set at a 45 degrees inclination using a 1mN Busek BET-1 electrospray thruster on a theoretical 6u CubeSat with an approximate weight of 10 kg. Synchronous orbits are a highly valued subset of science orbits around earth and other planets, so it is useful to analyze the capability of the system to obtain these orbits.

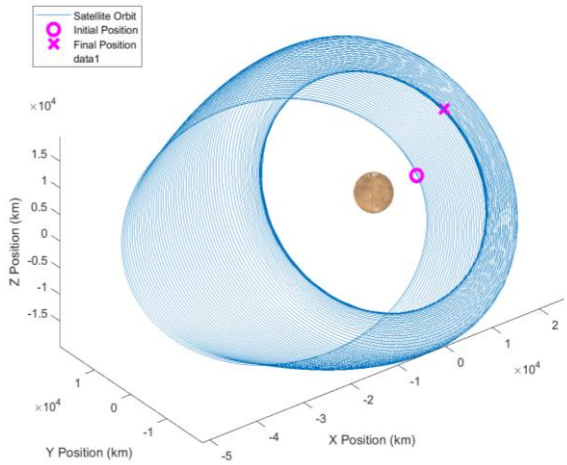

Figure 4. Controlled Transfer from high to zero eccentricity

The BET-1 electric propulsion system is most efficient when running at its full power of 1mN, therefore the control is constrained to run at this magnitude. The control law Equation 10 determined the direction of the control vector.

The starting injection orbit depends on the interplanetary trajectory and the mission details. The target orbit is AEO at 45 degrees inclination, as this GEO counterpart is a common target of science and communication missions. Arbitrary errors of 0.7 eccentricity, 10,000 km semi-major axis, and 3-degrees inclination were chosen to demonstrate the control, as this starting orbit models a known obtainable injection orbit.[6]

The maneuver using Lyapunov with efficiency-based gains completed in 90 days with an initial mass of 10kg and used 0.33 kg of fuel during the maneuver. The satellite then maintained the targeted orbital elements for an additional 200 days with 0.002 kg of fuel.

The inclination change completed first due to the relatively small error as seen in Fig. 5. The control then focused on simultaneously reducing eccentricity and semi-major axis before finishing the correction of the large semi-major axis error.

The thrust components for the span of 2 Martian days to obtain this controlled system can be seen in both the satellite centered coordinate system RSW and the inertial frame MCI coordinate system in Fig. 8.

A comparison to the Lyapunov controller with the efficiency gains turned off is shown in Table 1. Steady state (SS) errors for the controllers are based on the tolerance constraints given to the controller as to prevent oscillation about the target. This comparison to static gains shows the reduction in fuel usage at the cost of time. Indivual mission requirements would have to be determined to investigate if this increased fuel efficiency is worth the maneuver completion time.

Table 1: Comparison of control methods for maneuver only.

Cost Parameters	Lyapunov with efficiency	Lyapunov with constant gains [1,1,50]
Fuel Used	0.35 kg	0.37 kg
Maneuver Time	90 days	87 days
Average SS Error *[a, e, i]*	20 kilometers 0.001 0.03 degrees	25 kilometers 0.001 0.03 degrees

Of importance to note are effects that are ignored including atmospheric drag, which is considered negligible for Mars, and shadow effects due to the electric propulsion requiring large amounts of power. These can be designed around by including more power storage for the shadow effect and putting a constraint on the lower limit of the altitude, so the very thin Martian atmosphere will not have a recognizable effect.

Including oblatenness and third body gravity effects into the gauss variation equations used in the control input matrix could also increase the effectiveness of orbital element maintenance and small element error corrections. This inclusion would be relatively simple to implement as the effects would not have to be linearized in a non-linear Lyapunov control system.

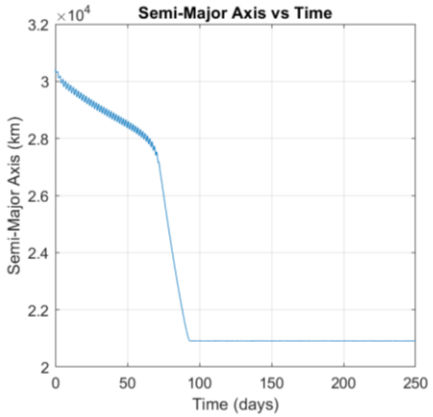

Figure 5. Semi-Major Axis Example transfer over 250 maintenance time-span

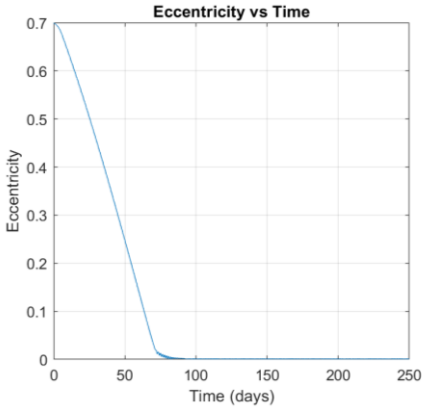

Figure 6. Example orbit transfer circularizing eccentricity.

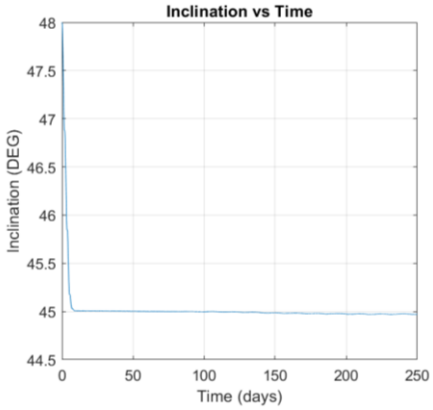

Figure 7. Inclination targeting of 45 degrees for Example transfer.

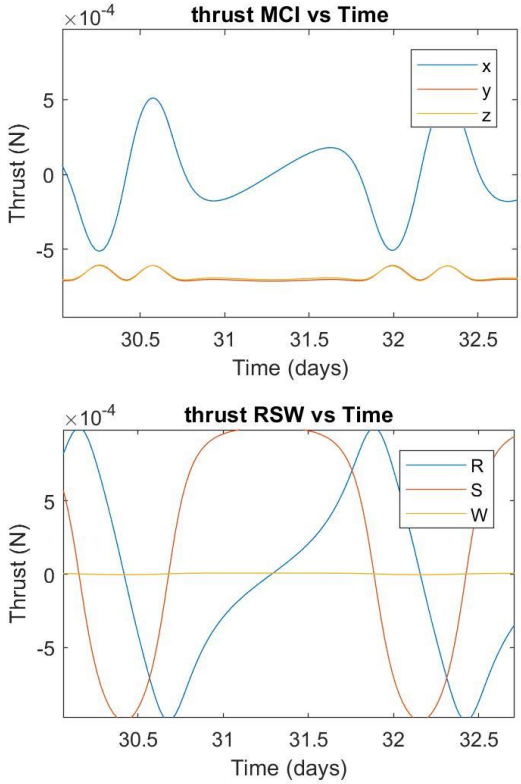

Figure 8. Thrust components produce by electric thruster for the controlled example simulation

CONCLUSION

The simulation of the system constructed here provides a detailed model of gravity perturbations and third body effects. Additionally, a control scheme is constructed that is simple to tune for specific low-thrust propulsion missions' mass and time requirements. Results for fuel use and transfer time span were found for example transfers and a thrust profile was constructed showing pointing vectors for a low-thrust propulsion system.

REFERENCES

1. Genova, A., Goossens, S., Lemoine, F. G., Mazarico, E., Neuman, G. A., Smith, D. E., Zuber, M. T., "Seasonal and static gravity field of Mars from MGS, Mars Odyssey and MRO radio science," Icarus, Vol. 272, 2016, pp. 228–245.
2. Vallado, D. A., Fundamentals of astrodynamics and applications, New York: Springer, 2007.

3. Naasz, B. J., “Classical Element Feedback for Spacecraft Orbital Maneuvers,” master’s thesis, Virginia Polytechnic Institute and State University, Blacksburg, Virginia, 2002.
4. SPICE Toolkit, Spacecraft Planet Instrument C-matrix Events Toolkit, Software Package, Ver. 1.0, NASA Navigation and Ancillary Information Facility, 2017.
5. Martin-Mur T., Gustafson E., Young B., “Interplanetary Cubesat Navigational Challenges,” International Symposium on Space Flight Dynamics.
6. Springmann, J., Kempke B., Cutler, J. & Bahcivan H., “Development and Initial Operations of The Rax-2 Cubesat,” The 4S symposium (2013).
7. S. De Florio, S. D'amico, and G. Radice. "Precise Autonomous Orbit Control in Low Earth Orbit", AIAA/AAS Astrodynamics Specialist Conference, Guidance, Navigation, and Control and Co-located Conferences,